IEEE Photonics Journal
An IEEE Photonics Society Publication

Open Access

Weak Scattering of Young's Diffractive Light Wave From a Spatially Deterministic Medium

Volume 8, Number 6, December 2016

Jia Li
Feinan Chen
Liping Chang

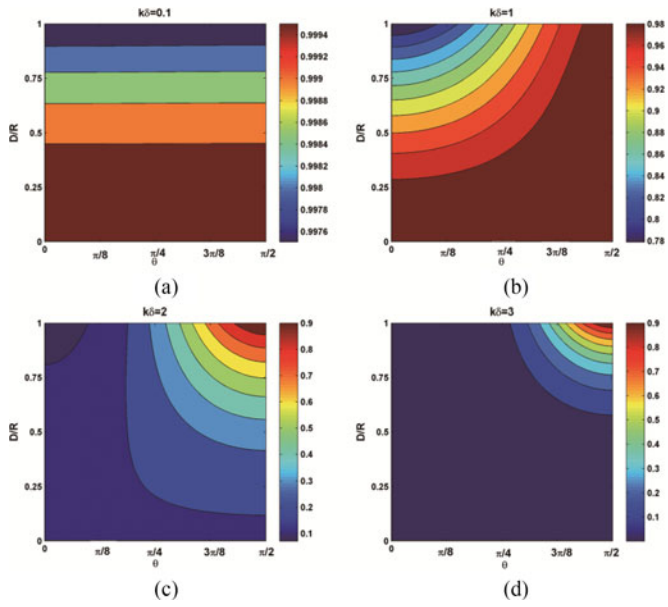

DOI: 10.1109/JPHOT.2016.2625518
1943-0655 © 2016 IEEE

Weak Scattering of Young's Diffractive Light Wave From a Spatially Deterministic Medium

Jia Li,[1,2] **Feinan Chen,**[3] **and Liping Chang**[2]

[1]Department of Physics, College of Arts and Sciences, University of Miami, Coral Gables, FL 33146 USA
[2]Institute of Fiber Optic Communication and Information Engineering, College of Information Engineering, Zhejiang University of Technology, Hangzhou 310023, China
[3]Photoelectric Measurement and Control Technology and Instrumentation Research Center, Institute of Applied Technology, Hefei Institutes of Physical Science, Chinese Academy of Sciences, Hefei 230031, China

DOI:10.1109/JPHOT.2016.2625518
1943-0655 © 2016 IEEE. Translations and content mining are permitted for academic research only. Personal use is also permitted, but republication/redistribution requires IEEE permission. See http://www.ieee.org/publications_standards/publications/rights/index.html for more information.

Manuscript received September 21, 2016; accepted November 1, 2016. Date of publication November 4, 2016; date of current version November 22, 2016. The work of J. Li was supported in part by the National Natural Science Foundation of China (NSFC) under Grant 61205121 and Grant 61304124 and in part by the Natural Science Foundation of Zhejiang Province under Grant LY13F010009 and Grant LY15F050012. The work of F. Chen was supported by the NSFC under Grant 11504383. Corresponding author: J. Li (e-mail: jxl1180@miami.edu).

Abstract: We study the modeling of the scattering of Young's diffractive light wave from a 3-D medium of which the refractive index is a deterministic function of position. Within the validity of the first-order Born approximation, the spectral density of the scattered field is derived as the analytic form. It is shown that the scattering angle and effective radius of the scattering potential account for the substantial effects on the spectral density profiles of the scattered field. It is also revealed that Young's pinhole parameter can affect the spectral density distribution of the scattered field. Our findings may be significant for the determination of structural parameters of an unknown scatterer.

Index Terms: Young's pinhole, Born approximation, scattering potential.

1. Introduction

It has been well known that the spatial degree of coherence (DOC) of a partially coherent field can be determined by the interference experiment. In such a case, the Young's double-pinholes [1], [2] were commonly used to measure the DOC of an optical field. It has been reported that the DOC of a random optical field can be measured by obtaining the average intensity at pinholes and visibility of the interference image generated in a far-zone observation plane [1]. A spectral interference law governing behaviors of the Stokes parameters was introduced under the frame of the Young's double-pinhole experiment [3]. It was verified that the DOC of an electromagnetic wave diffracting from Young's pinholes can be obtained by measuring the visibility of intensity fringes and contrasts of the polarization Stokes parameters [4]. Then, the interference law has been shown to be a great advantage for the polarization interferometry and analysis of a random, statistical field. The scattering properties of the spectral density, spectral DOC, and spectral degree of polarization (DOP) of a Young's interference wave from a spatially random medium were investigated, respectively, in [5]. The reversible optical transformation law was introduced to achieve the maximum visibility of

the transmitted wave from Young's pinholes [6]. It was obtained that the light trespassing a pinhole and interacting with a non-absorbing anisotropic medium can exhibit the enhanced imaging visibility. Based on the beam coherence-polarization (BCP) matrix, the conditions for the invariance of the polarization of an electromagnetic beam propagating through a Young interferometer were obtained [7]. Besides, polarization singularities were studied for the beams transmitting though Young's double slits [8]. It was revealed that the spectral shifts and spectral switches of a partially coherent pulsed beam from Young's pinholes can be flexibly controlled by appropriately tuning the beam parameters and pinhole structure [9]. Topological properties of the vectorial fields transmitting through Young's pinholes were also investigated [10]. Studies were performed on beam correlation properties by using a pinhole array to filter the beam intensity pattern [11]. Recently, Friberg *et al.* introduced the modified Young's interferometer that can provide a measure of the DOC of a polychromatic light, regardless of the spectral nature of radiation [12].

The above literature covered almost overall aspects of the theoretical and experimental investigations of the Young's double pinholes. However, the property of the diffractive wave through Young's pinholes interacting with a spatially deterministic or random scatterer is still an unsolved problem. According to our knowledge, no study has been done to address this problem. In this paper, we focus on modeling the scattering theory of a Young's diffractive wave from a spatially deterministic medium. We assume that the scattering of the diffractive wave from the scatterer is so weak; hence, the first-order Born approximation can be applied to treat the scattering process. The cross-spectral density function (CSDF) and spectral density of the scattered field are derived in analytic expressions, respectively. Numerical results are exhibited to reveal the influences of the scattering angle, scattering potential profile and YPP on shaping the spectral density distribution of the scattered field.

2. CSDF of the Diffractive Wave Transmitting Through Young's Double Pinholes

To begin with, we first derive the CSDF of the diffractive wave through Young's pinholes. To this effort, we assume that a scalar plane wave propagates along z axis and illuminates at a Young's pinhole screen. After transmitting through pinholes, the diffractive wave subsequently propagates until it interacts with a 3-D scatterer with a finite volume D. Let $\langle U^{(i)}(\vec{\rho}_j)\rangle$ $(j = 1, 2)$ be the ensemble average of the electric field of the incident plane wave. We also assume that the screen A with pinholes denoted by $Q(\vec{\rho}_1)$ and $Q(\vec{\rho}_2)$ is placed perpendicular to z axis. The diffractive wave propagates and scatters upon a medium of which the spatial refractive index is a deterministic function of position, and the distance between the scatterer and screen A is R. $\vec{\rho}_1$ and $\vec{\rho}_2$ are position vectors of the incident wave, φ_1 and φ_2 are azimuthal angles corresponding to the position vectors. $P(\vec{\mathbf{r}}_1)$, $P(\vec{\mathbf{r}}_2)$ are the points where the diffractive wave interacts with the medium. The unit vectors $\vec{\mathbf{s}}_1$ and $\vec{\mathbf{s}}_2$ are position vectors of the scattered field, θ_1 and θ_2 are scattering angles. Recalling the Young's interference law, the diffractive field at $P(\vec{r}_1)$, $P(\vec{r}_2)$ can be represented by the matrix form [1], [5]

$$\begin{pmatrix} U^{(f)}\left(\vec{\mathbf{r}}_1'\right) \\ U^{(f)}\left(\vec{\mathbf{r}}_1'\right) \end{pmatrix} = \begin{pmatrix} K_{11} & K_{12} \\ K_{21} & K_{22} \end{pmatrix} \begin{pmatrix} U^{(i)}\left(\vec{\rho}_1\right) \\ U^{(i)}\left(\vec{\rho}_2\right) \end{pmatrix} \tag{1}$$

where $\langle U^{(i)}(\vec{\rho}_j)\rangle$ is the electric field of the incident plane wave that has the monochromatic spectral profile

$$U^{(i)}\left(\vec{\rho}_j\right) = A_0 \exp\left(-ik\vec{\mathbf{s}}_0 \cdot \vec{\rho}_j\right), \quad (j = 1,\ 2) \tag{2}$$

and $K_{\alpha\beta}$ is the propagator given by the form

$$K_{\alpha\beta} = -\frac{ik}{2\pi}\frac{\exp\left(ikR_{\alpha\beta}\right)}{R_{\alpha\beta}}dS, \quad (\alpha,\ \beta = 1,\ 2). \tag{3}$$

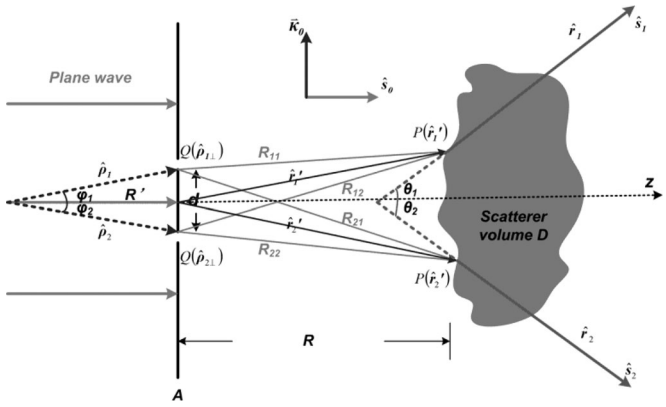

Fig. 1. Schematic diagram for the light diffracting through Young's pinholes and interacting with a spatially deterministic medium with a finite volume *D*.

In (3), $R_{\alpha\beta}$ is the distance between $P(\vec{\mathbf{r}}_\alpha')$ and $Q(\vec{\boldsymbol{\rho}}_\beta)$, dS is the pinhole area, and $\lambda = 2\pi/k$ denotes the wavelength of the incident plane wave. From (1) and hereafter, the dependence of the electric field on frequency ω is omitted but implied. By substituting from (2) and (3) into (1), the resultant diffractive fields show the form

$$U^{(f)}\left(\vec{\mathbf{r}}_1'\right) = -\frac{ikA_0}{2\pi}dS\left[\frac{\exp\left(ikR_{11} - ik\vec{\mathbf{s}}_0\cdot\vec{\boldsymbol{\rho}}_1\right)}{R_{11}} + \frac{\exp\left(ikR_{12} - ik\vec{\mathbf{s}}_0\cdot\vec{\boldsymbol{\rho}}_2\right)}{R_{12}}\right] \tag{4}$$

$$U^{(f)}\left(\vec{\mathbf{r}}_2'\right) = -\frac{ikA_0}{2\pi}dS\left[\frac{\exp\left(ikR_{21} - ik\vec{\mathbf{s}}_0\cdot\vec{\boldsymbol{\rho}}_1\right)}{R_{21}} + \frac{\exp\left(ikR_{22} - ik\vec{\mathbf{s}}_0\cdot\vec{\boldsymbol{\rho}}_2\right)}{R_{22}}\right]. \tag{5}$$

Next, let us recall the definition of the CSDF of the diffractive field specified at points $\vec{\mathbf{r}}_1'$ and $\vec{\mathbf{r}}_2'$ [13]

$$W^{(f)}\left(\vec{\mathbf{r}}_1', \vec{\mathbf{r}}_2'\right) = \left\langle U^{(f)*}\left(\vec{\mathbf{r}}_1'\right) U^{(f)}\left(\vec{\mathbf{r}}_2'\right)\right\rangle \tag{6}$$

where the asterisk denotes complex conjugate, the angular bracket represents the ensemble average over the entire diffractive field. We assume that $R_{\alpha\beta}$ is sufficiently large compared with the wavelength of the incident wave. This means that $R_{\alpha\beta}$ in the denominator of (4) and (5) can be approximated to a constant R, i.e.,

$$R_{\alpha\beta} \approx R, \quad (\alpha,\ \beta = 1,\ 2). \tag{7}$$

By substituting from (4) and (5) into (6) and using (7), the CSDF of the diffractive wave can be given by

$$W^{(f)}\left(\vec{\mathbf{r}}_1', \vec{\mathbf{r}}_2'\right) = \left(\frac{kdS}{2\pi R}\right)^2 I_0\left\{\exp\left[ik\left(R_{21} - R_{11}\right) + \exp\left[ik\left(R_{22} - R_{12}\right)\right]\right] + \exp\left[ik\left(R_{21} - R_{12}\right)\right.\right.$$
$$\left.\left. + ik\left(\left|\vec{\boldsymbol{\rho}}_2\right|\cos\varphi_2 - \left|\vec{\boldsymbol{\rho}}_1\right|\cos\varphi_1\right)\right]\right\} + \exp\left[ik\left(R_{22} - R_{11}\right) + ik\left(\left|\vec{\boldsymbol{\rho}}_1\right|\cos\varphi_1 - \left|\vec{\boldsymbol{\rho}}_2\right|\cos\varphi_2\right)\right]\right\}, \tag{8}$$

where $I_0 = A_0^2$ is the amplitude resulting from the incident wave. We assume that the pinholes are symmetrically distributed with respect to z axis, as shown in Fig. 1. Accordingly, the following relation is obtained

$$\left|\vec{\boldsymbol{\rho}}_1\right|\cos\varphi_1 = \left|\vec{\boldsymbol{\rho}}_2\right|\cos\varphi_2 = R'. \tag{9}$$

Furthermore, we also assume that the diffractive wave from pinholes paraxially propagates along z axis until interacting with the medium. As a result, we may approximate $R_{\alpha\beta}$ in the exponential terms of (8) to the following forms [5]:

$$R_{21} - R_{11} \approx \frac{(r'_{2\perp} - r'_{1\perp})\, d}{2R} \tag{10}$$

$$R_{22} - R_{12} \approx \frac{(r'_{2\perp} - r'_{1\perp})\, d}{2R} \tag{11}$$

$$R_{12} - R_{11} \approx \frac{r'_{1\perp} d}{R} \tag{12}$$

$$R_{22} - R_{21} \approx \frac{r'_{2\perp} d}{R} \tag{13}$$

where $r'_{j\perp} = |\vec{\mathbf{r}}'_{\mathbf{j}\perp}|$ is the modulus of the projective vector, and d denotes the distance between pinholes. In particular, here, we introduce the unit vector $\vec{\kappa}_{\mathbf{0}}$ which is perpendicular to the incident unit vector $\vec{\mathbf{s}}_{\mathbf{0}}$ (shown in Fig. 1). As a result, we can obtain the following vectorial relations:

$$r'_{1\perp} = \vec{\mathbf{r}}_{\mathbf{1}}' \cdot \vec{\kappa}_{\mathbf{0}}, \qquad r'_{2\perp} = -\vec{\mathbf{r}}_{\mathbf{2}}' \cdot \vec{\kappa}_{\mathbf{0}}, \qquad \vec{\kappa}_{\mathbf{0}} \cdot \vec{\mathbf{s}}_{\mathbf{0}} = 0. \tag{14}$$

By substituting from (10)–(13) into (8) and using (9) and (14), the resultant CSDF of the diffractive wave yields the simplified form

$$W^{(f)}\left(\vec{\mathbf{r}}_{\mathbf{1}}', \vec{\mathbf{r}}_{\mathbf{2}}'\right) = \left(\frac{kdS}{2\pi R}\right)^2 I_0 \left\{2\exp\left[-i\frac{kd}{2R}\left(\vec{\mathbf{r}}_{\mathbf{1}}' + \vec{\mathbf{r}}_{\mathbf{2}}'\right) \cdot \vec{\kappa}_{\mathbf{0}}\right] + \exp\left[i\frac{kd}{2R}\left(\vec{\mathbf{r}}_{\mathbf{2}}' - \vec{\mathbf{r}}_{\mathbf{1}}'\right) \cdot \vec{\kappa}_{\mathbf{0}}\right] + \exp\left[-i\frac{kd}{2R}\left(\vec{\mathbf{r}}_{\mathbf{2}}' - \vec{\mathbf{r}}_{\mathbf{1}}'\right) \cdot \vec{\kappa}_{\mathbf{0}}\right]\right\}. \tag{15}$$

From observing (15), we can conclude that the CSDF of the diffractive wave is the summation of three independent terms: the first term within the bracket on the right-hand side of the equation represents the diffractive component from each pinhole, while the second and third terms are attributed to the interference components generated from Young's pinholes. Equation (15) provides a fundamental basis for studying the scattering properties of the diffractive wave from a spatially deterministic medium.

3. Scattering of the Diffractive Wave From a Spatially Deterministic Medium

In the previous section, we derived the analytic form for the CSDF of the diffractive wave through Young's pinholes. In what follows, we will handle with the interaction between the diffractive wave and the spatially deterministic medium. Within the validity of the first-order Born approximation, the far-zone CSDF of a scattered field specified at points $\vec{\mathbf{r}}_{\mathbf{1}}$ and $\vec{\mathbf{r}}_{\mathbf{2}}$ can be represented by the integral form [14]–[19]

$$W^{(s)}\left(\vec{\mathbf{r}}_{\mathbf{1}}, \vec{\mathbf{r}}_{\mathbf{2}}\right) = \frac{\exp\left[ik\left(r_2 - r_1\right)\right]}{r_1 r_2} \int_D \int_D W^{(f)}\left(\vec{\mathbf{r}}_{\mathbf{1}}', \vec{\mathbf{r}}_{\mathbf{2}}'\right) F^*\left(\vec{\mathbf{r}}_{\mathbf{1}}'\right) F\left(\vec{\mathbf{r}}_{\mathbf{2}}'\right) \exp\left(ik\vec{\mathbf{s}}_{\mathbf{1}} \cdot \vec{\mathbf{r}}_{\mathbf{1}}' - ik\vec{\mathbf{s}}_{\mathbf{2}} \cdot \vec{\mathbf{r}}_{\mathbf{2}}'\right) d^3 r_1' d^3 r_2' \tag{16}$$

where

$$F\left(\vec{\mathbf{r}}'\right) = \frac{k^2}{4\pi}\left[\mu\left(\vec{\mathbf{r}}'\right) - 1\right] \tag{17}$$

is the scattering potential of the medium, $\mu(\vec{\mathbf{r}}')$ denotes the electric permittivity of the medium and is related to the spatial refractive index as $\mu(\vec{\mathbf{r}}') = n^2(\vec{\mathbf{r}}')$ [20], [21]. The subscript D in (16) implies that integration is taken over the entire scatterer volume. By substituting (15) into (16), the CSDF

of the scattered field is given by

$$W^{(s)}\left(r\vec{\mathbf{s}}_1, r\vec{\mathbf{s}}_2\right) = \frac{I_0}{r^2}\left(\frac{kdS}{2\pi R}\right)^2 \left\{2\left[\int_D F\left(\vec{\mathbf{r}}_1'\right)\exp\left(i\frac{kd}{2R}\vec{\mathbf{r}}_1'\cdot\vec{\kappa}_0 - ik\vec{\mathbf{s}}_1\cdot\vec{\mathbf{r}}_1'\right)d^3r_1'\right]^*\right.$$
$$\times\int_D F\left(\vec{\mathbf{r}}_2'\right)\exp\left(-i\frac{kd}{2R}\vec{\mathbf{r}}_2'\cdot\vec{\kappa}_0 - ik\vec{\mathbf{s}}_2\cdot\vec{\mathbf{r}}_2'\right)d^3r_2' + \left[\int_D F\left(\vec{\mathbf{r}}_1'\right)\exp\left(i\frac{kd}{2R}\vec{\mathbf{r}}_1'\cdot\vec{\kappa}_0 - ik\vec{\mathbf{s}}_1\cdot\vec{\mathbf{r}}_1'\right)d^3r_1'\right]^*$$
$$\times\int_D F\left(\vec{\mathbf{r}}_2'\right)\exp\left(i\frac{kd}{2R}\vec{\mathbf{r}}_2'\cdot\vec{\kappa}_0 - ik\vec{\mathbf{s}}_2\cdot\vec{\mathbf{r}}_2'\right)d^3r_2' + \left[\int_D F\left(\vec{r}_1'\right)\exp\left(-i\frac{kd}{2R}\vec{\mathbf{r}}_1'\cdot\kappa_0 - ik\vec{\mathbf{s}}_1\cdot\vec{\mathbf{r}}_1'\right)d^3r_1'\right]^*$$
$$\left.\times\int_D F\left(\vec{\mathbf{r}}_2'\right)\exp\left(-i\frac{kd}{2R}\vec{\mathbf{r}}_2'\cdot\vec{\kappa}_0 - ik\vec{\mathbf{s}}_2\cdot\vec{\mathbf{r}}_2'\right)d^3r_2'\right\}. \tag{18}$$

By performing the integrations in (18), it follows that the CSDF of the scattered field gives arise to the form

$$W^{(s)}\left(r\vec{\mathbf{s}}_1, r\vec{\mathbf{s}}_2\right) = \frac{I_0}{r^2}\left(\frac{kdS}{2\pi R}\right)^2 \left\{2\tilde{F}^*\left[k\left(\vec{\mathbf{s}}_1 - \frac{d}{2R}\vec{\kappa}_0\right)\right]\tilde{F}\left[k\left(\vec{\mathbf{s}}_2 + \frac{d}{2R}\vec{\kappa}_0\right)\right] + \tilde{F}^*\left[k\left(\vec{\mathbf{s}}_1 - \frac{d}{2R}\vec{\kappa}_0\right)\right]\right.$$
$$\left.\times\tilde{F}\left[k\left(\vec{\mathbf{s}}_2 - \frac{d}{2R}\vec{\kappa}_0\right)\right] + \tilde{F}^*\left[k\left(\vec{\mathbf{s}}_1 + \frac{d}{2R}\vec{\kappa}_0\right)\right]\tilde{F}\left[k\left(\vec{\mathbf{s}}_2 + \frac{d}{2R}\vec{\kappa}_0\right)\right]\right\} \tag{19}$$

where

$$\tilde{F}\left(\vec{\mathbf{K}}_{\mathbf{j}}^{\pm}\right) = \int_D F\left(\vec{\mathbf{r}}'\right)\exp\left[-i\vec{\mathbf{K}}_{\mathbf{j}}^{\pm}\cdot\vec{\mathbf{r}}'\right]d^3r', \qquad (j = 1,\ 2) \tag{20}$$

is the 3-D Fourier transform of the scattering potential, and

$$\vec{\mathbf{K}}_{\mathbf{j}}^{\pm} = k\left(\vec{\mathbf{s}}_{\mathbf{j}} \pm \frac{d}{2R}\vec{\kappa}_0\right), \qquad (j = 1,\ 2) \tag{21}$$

is analogous to the momentum transfer vector in a quantum field [14]–[21]. Followed by (19), we can readily obtain the spectral density of the scattered field at a point $\vec{\mathbf{r}}$

$$S^{(s)}\left(r\vec{\mathbf{s}}\right) = W^{(s)}\left(r\vec{\mathbf{s}}, r\vec{\mathbf{s}}\right) = \frac{I_0}{r^2}\left(\frac{kdS}{2\pi R}\right)^2 \left\{\left|\tilde{F}\left[k\left(\vec{\mathbf{s}} - \frac{d}{2R}\vec{\kappa}_0\right)\right]\right|^2 + \left|\tilde{F}\left[k\left(\vec{\mathbf{s}} + \frac{d}{2R}\vec{\kappa}_0\right)\right]\right|^2\right.$$
$$\left. + 2\tilde{F}^*\left[k\left(\vec{\mathbf{s}} - \frac{d}{2R}\vec{\kappa}_0\right)\right]\tilde{F}\left[k\left(\vec{\mathbf{s}} + \frac{d}{2R}\vec{\kappa}_0\right)\right]\right\}. \tag{22}$$

Equation (22) shows that the spectral density of the scattered field not only depends on the scattering angle and scattering potential profile of the medium but relates to the YPP, i.e., *d/R*, as well. In our following discussion, we will show a typical example, the scattering of light from a medium with the Gaussian scattering potential. Numerical results will be presented to reveal the effects of the potential's profile and YPP on the scattered spectral density in the far field.

4. Numerical Results and Discussions

In this section, numerical computations are performed to study the spectral density distributions of the light scattered from the spatially deterministic medium. Discussions are held on analyzing the influences of the scattering angle, scattering the potential profile of the medium and YPP on the scattered intensities in the far field. For this purpose, we assume that the scattering potential has the Gaussian profile [21], [22]

$$F\left(\vec{\mathbf{r}}'\right) = \left(\frac{\omega}{c}\right)^2 \frac{A}{\left(2\pi\delta^2\right)^{3/2}}\exp\left[-\frac{r'^2}{2\delta^2}\right] \tag{23}$$

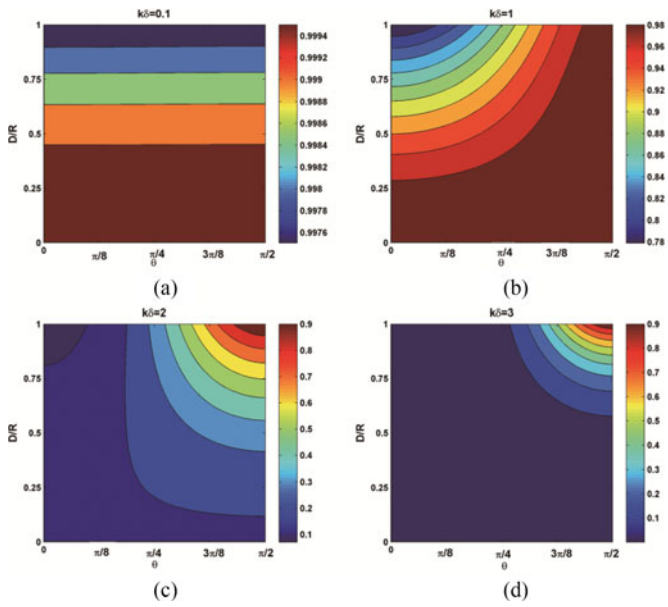

Fig. 2. Normalized spectral density distributions of the scattered field versus the scattering angle $\theta \in [0,\ \pi/2]$ and d/R for different effective widths of the scattering potential. (a) $k\delta = 0.1$, (b) $k\delta = 1$, (c) $k\delta = 2$, (d) $k\delta = 3$.

where A and δ are positive constants that may depend on frequency. Then, it follows from (20) and (23) that

$$\tilde{F}\left(\vec{\mathbf{K}}_{\mathbf{j}}^{\pm}\right) = \left(\frac{\omega}{c}\right)^2 A \exp\left[-\left|\vec{\mathbf{K}}_{\mathbf{j}}^{\pm}\right|^2 \delta^2/2\right], \qquad (j = 1,\ 2). \tag{24}$$

With the help of (21), (24) can be rewritten as the alternative form

$$\tilde{F}\left(\vec{\mathbf{K}}_{\mathbf{j}}^{\pm}\right) = \left(\frac{\omega}{c}\right)^2 A \exp\left[-\frac{k^2\delta^2}{2}\left(1 + \frac{d^2}{4R^2} \pm \frac{d}{R}\sin\theta_j\right)\right], \qquad (j = 1,\ 2). \tag{25}$$

The spectral density of the scattered field can be obtained by substituting from (25) into (22)

$$S^{(s)}\left(r\vec{\mathbf{s}}, \omega\right) = \frac{A^2 I_0}{r^2}\left(\frac{k^3 dS}{2\pi R}\right)^2 \left\{2\exp\left[-k^2\delta^2\left(1 + \frac{d^2}{4R^2}\right)\right] + \exp\left[-k^2\delta^2\left(1 + \frac{d^2}{4R^2} - \frac{d}{R}\sin\theta\right)\right] + \exp\left[-k^2\delta^2\left(1 + \frac{d^2}{4R^2} + \frac{d}{R}\sin\theta\right)\right]\right\}. \tag{26}$$

From observing (26), we can conclude that the spectral density of the scattered field transmitting through Young's pinholes is dependent on the scattering angle, scattering potential distribution of the medium and YPP. Fig. 2 reveals the dependence of the normalized spectral density of the scattered field on the effective width δ, d/R and the scattering angle θ. For the sufficiently small effective width, e.g. $k\delta = 0.1$, the scattering angle has negligible influence on the spectral density of the scattered field, as shown by Fig. 2(a). The scattered intensity is substantially enhanced by decreasing d/R, attributing to the aperture-average effect produced by Young's pinholes. Furthermore, when the effective width of the scattering potential increases to $k\delta = 1$, the spectral density of the scattered field becomes non-uniform and its value is enhanced by increasing the scattering angle. In particular, when the effective width becomes sufficiently large, e.g., $k\delta = 2$ or $k\delta = 3$, the peak position of the

scattered spectral density shifts to a very large scattering direction. These phenomena are shown in Figs. 2(c)-2(d).

Our results can be utilized to generate the desired spectral density profiles of the scattered field. They also provide a flexible approach for determination of structural parameters of a 3-D object. Followed by (22) and (26), it is feasible to generate the desired spectral density of the scattered field by tuning the YPP or effective width of the scattering potential. The presented graph is significant for shaping the controllable peak profile of a scattered field. In addition, the spectral density of the scattered field commonly carries essential information of the scattering potential of a deterministic medium. With the help of (26), we can determine the scattering potential of a medium by knowing the scattered spectral density in the far field. Future studies related to our work include the experimental verification of the theoretical results, which might be presented in our future publication.

5. Conclusion

The weak scattering of a Young's diffractive wave from a spatially deterministic medium is studied. Within the validity of the first-order Born approximation, analytic formulas are derived for the CSDF and spectral density of the far-zone scattered field. Assuming that the scattering potential of the medium has the Gaussian profile, numerical graphs are presented to reveal the dependences of the scattered spectral density on the medium's parameters and pinhole structure. It is shown that the scattering angle leads no influence on sharping the spectral density of the scattered field when the effective width of the scattering potential is sufficiently small. However, the scattering angle effect becomes evident when the effective width is comparable with or larger than the incident wavelength. Moreover, the position of peak intensity of the scattered field can be shifted to a very large scattering direction by suitably choosing the effective width and YPP. The theoretical results in our paper provide a useful approach to determine structural parameters of a 3-D object by measuring the spectral density distribution of the scattered field.

References

[1] L. Mandel and E. Wolf, *Optical Coherence and Quantum Optics*. Cambridge, U.K.: Cambridge Univ. Press, 1995.
[2] O. V. Angelsky, C. Y. Zenkova, M. P. Gorsky, and N. V. Gorodyns'ka, "Feasibility of estimating the degree of coherence of waves at the near field," *Appl. Opt.*, vol. 48, no. 15, pp. 2784–2788, 2009.
[3] T. Setàlà, J. Tervo, and A. T. Friberg, "Stokes parameters and polarization contrasts in Young's interference experiment," *Opt. Lett.*, vol. 31, no. 14, pp. 2208–2210, 2006.
[4] T. Setàlà, J. Tervo, and A. T. Friberg, "Contrasts of Stokes parameters in Young's interference experiment and electromagnetic degree of coherence," *Opt. Lett.*, vol. 31, no. 18, pp. 2669–2671, 2006.
[5] Y. Li, H. Lee, and E. Wolf, "Spectra, coherence and polarization in Young's interference pattern formed by stochastic electromagnetic beams," *Opt. Commun.*, vol. 265, no. 1, pp. 63–72, 2006.
[6] F. Gori, M. Santarsiero, and R. Borghi, "Maximizing Young's fringe visibility through reversible optical transformations," *Opt. Lett.*, vol. 32, no. 6, pp. 588–590, 2007.
[7] M. Santarsiero, "Polarization invariance in a Young interferometer," *J. Opt. Soc. Amer. A*, vol. 24, no. 11, pp. 3493–3499, 2007.
[8] X. Lian and B. Lù, "Polarization singularities in Young's two-slit experiment," *Opt. Commun.*, vol. 284, no. 22, pp. 5253–5258, 2011.
[9] C. Ding, B. Lù, and L. Pan, "Spectral shifts and spectral switches of spatially and spectrally partially coherent pulsed beams in Young's interference experiment," *Opt. Commun.*, vol. 282, no. 3, pp. 413–422, 2009.
[10] Y. Li *et al.*, "Young's two-slit interference of vector light fields," *Opt. Lett.*, vol. 37, no. 11, pp. 1790–1792, 2012.
[11] D. F. Siriani, "Beyond young's experiment: Time-domain correlation measurement in a pinhole array," *Opt. Lett.*, vol. 38, no. 6, pp. 857–859, 2013.
[12] K. Saastamoinen, J. Tervo, J. Turunen, P. Vahimaa, and A. T. Friberg, "Spatial coherence measurement of polychromatic light with modified Young's interferometer," *Opt. Exp.*, vol. 21, no. 4, pp. 4061–4071, 2013.
[13] E. Wolf, "Unified theory of coherence and polarization of random electromagnetic beams," *Phys. Lett. A*, vol. 312, no. 5/6, pp. 263–267, 2003.
[14] J. Chen *et al.*, "Coherence properties of the scattered electromagnetic field generated by anisotropic media," *Opt. Commun.*, vol. 285, no. 19, pp. 3955–3960, 2012.
[15] X. Du and D. Zhao, "Reciprocity relations for scattering from quasi-homogeneous anisotropic media," *Opt. Commun.*, vol. 284, no. 16/17, pp. 3808–3810, 2011.
[16] X. Du and D. Zhao, "Scattering of light by Gaussian-correlated quasi-homogeneous anisotropic media," *Opt. Lett.*, vol. 35, no. 3, pp. 384–386, 2010.

[17] Y. Xin, Y. Chen, Q. Zhao, M. Zhou, and X. Yuan, "Changes of spectrum of light scattering on quasi-homogeneous random media," *Proc. SPIE*, vol. 6786, 2007, Art. no. 67864S.
[18] T. D. Visser, D. G. Fischer, and E. Wolf, "Scattering of light from quasi-homogeneous sources by quasi-homogeneous media," *J. Opt. Soc. Amer. A*, vol. 23, no. 7, pp. 1631–1638, 2006.
[19] X. Du and D. Zhao, "Spectral shifts produced by scattering from rotational quasi-homogeneous anisotropic media," *Opt. Lett.*, vol. 36, no. 24, pp. 4749–4751, 2011.
[20] Z. Tong and O. Korotkova, "Theory of weak scattering of stochastic electromagnetic fields from deterministic and random media," *Phys. Rev. A*, vol. 82, no. 3, 2010, Art. no. 033836.
[21] M. Lahiri and E. Wolf, "Spectral changes of stochastic beams scattered on a deterministic medium," *Opt. Lett.*, vol. 37, no. 13, pp. 2517–2519, 2012.
[22] D. Zhao, O. Korotkova, and E. Wolf, "Application of correlation-induced spectral changes to inverse scattering," *Opt. Lett.*, vol. 32, no. 24, pp. 3483–3485, 2007.